Supporting Information

To the paper entitled

Enhancement of spin-crossover cooperativity mediated by lone pair–π interactions and halogen bonding

N. Nassirinia, S. Amani, Simon J. Teat, Olivier Roubeau,* and P. Gamez*

Table of Contents

Preparation of 2-chloro-4-(*N*,*N*-(2-pyridyl)amino)-6-(pentafluorophenoxy)-(1,3,5)triazine) (L1)

L1 was prepared in two steps applying the following procedure:

- First step: synthesis of 4,6-dichloro-*N*,*N*-di(pyridin-2-yl)-1,3,5-triazin-2-amine
  2.7 g (14.60 mmol) of 2,4,6-trichloro-{1,3,5}-triazine (cyanuric chloride) were dissolved in 100 mL of THF. Next, one equivalent (2.55 mL, 1.89 g; 14.60 mmol) of *N*,*N*-diisopropylethylamine (DIPEA) was added under stirring, and the resulting yellow solution was cooled to 0 °C using an ice bath. Subsequently, a solution of 2,2'-dipyridylamine (2.49 g; 14.60 mmol) in 25 mL of THF was added dropwise at 0 °C; After completion of the addition, the ice bath was removed and the reaction mixture was further stirred for one hour. The yellow precipitate obtained (*i.e*. hydrochloride salt of DIPEA) was eliminated by filtration. The solvent was then evaporated under reduced pressure, and the resulting crude compound was purified by column chromatography on silica gel with ethyl acetate as the eluent. 2.55 g (7.99 mmol, Yield = 55%) of pure 4,6-dichloro-*N*,*N*-di(pyridin-2-yl)-1,3,5-triazin-2-amine were obtained as a white powder. ^{1}H NMR (300 MHz, $CDCl_3$, room temp.): δ = 7.27–7.32 (m, 2H), 7.54 (dt, *J* = 8.1 Hz, *J* = 0.9 Hz, 2H), 7.85 (ddd, *J* = 8.1 Hz, *J* = 7.5 Hz, *J* = 2 Hz, 2H), 8.50 (ddd, *J* = 4.9 Hz, *J* = 1.9 Hz, *J* = 0.8 Hz, 2H) ppm. MS (ESI$^+$): m/z = 319.3 $[M + H]^+$ (319.03 calculated). IR (KBr): $\bar{\nu}$ = 1586 (s), 1551 (br), 1489 (s), 1462 (s), 1430 (s), 1325 (m), 1218(s), 1182 (s), 839 (s), 796 (m), 776 (m), 746 (m), 666 (m) cm^{-1}.
- Second step: synthesis of 2-chloro-4-(*N*,*N*-(2-pyridyl)amino)-6-(pentafluorophenoxy)-(1,3,5)triazine) (**L1**)
  1.00 g (3.13 mmol) of 4,6-dichloro-*N*,*N*-di(pyridin-2-yl)-1,3,5-triazin-2-amine was dissolved in 50 mL of THF. Next, one equivalent (0.405 g; 3.13 mmol) of DIPEA was added under stirring at room temperature. Subsequently, 0.576 g (3.13 mmol) of pentafluorophenol was added to the solution and the reaction mixture was stirred for 2 hours. The resulting yellow precipitate was separated by filtration, and the solvent was evaporated under reduced pressure. The crude product was purified by column chromatography on silica gel using n-hexane:ethyl acetate (1:2) as the eluent. 0.7 g (1.5 mmol, Yield = 48%) of **L1** was obtained as a white powder. ^{1}H NMR (300 MHz, $CDCl_3$, room temp.): δ = 7.20–7.26 (m, 2H), 7.52 (d, *J* = 8.1 Hz, 2H), 7.8 (td, *J* = 7.8 Hz, *J* = 1.9 Hz, 2H), 8.47–8.42 (m, 2H) ppm. MS (ESI$^+$): m/z =505.0; $[M+ K]^+$ (505). IR (KBr): $\bar{\nu}$ = 1656 (m), 1590 (br), 1561 (br), 1516 (br), 1470 (s), 1426(s), 1366(m), 1310(m), 1267 (m), 1231(s), 1151 (m), 1083 (w), 1022 (s), 995(s), 822(w), 802(m), 774(m), 739(m), 682(m), 664(w), 621(w), 537(w), 504(w) cm^{-1}.

Preparation of *trans*-$[Fe(L_1)_2(SCN)_2]\cdot 2CH_3OH$ (1)

A methanolic solution (5 mL) of KNCS (0.019 g; 0.2 mmol) was added to an aqueous solution (2 mL) of $FeSO_4\cdot 7H_2O$ (0.028 g, 0.1 mmol) under stirring. After 15 min, the precipitate of K_2SO_4 was removed by filtration and ascorbic acid (5 mg) was added to the filtrate to prevent oxidation of iron(II) to iron(III). Subsequently, a solution of **L1** (0.093 g, 0.2 mmol) in dichloromethane (15 mL) was added dropwise under stirring. The resulting yellow reaction mixture was filtered and the filtrate was left unperturbed for the slow evaporation of the solvent. Small yellow single crystals, suitable for X-ray diffraction studies, formed after 2 h (Yield: 0.098 g, 0.077 mmol, 77 %). $C_{40}H_{16}Cl_2F_{10}FeN_{14}O_2S_2$ (**1**–$2CH_3OH$) (1105.51): calcd. C 43.46, H 1.46, N 17.74; found C 43.39, H 1.60, N 17.60. IR (KBr): $\bar{\nu}$ = 3441(m), 3068 (w), 2062 (s), 1655 (w), 1602 (m), 1581 (m), 1564 (m), 1514 (s), 1472 (m), 1438 (m),

1365 (s), 1313 (m), 1240 (m), 1126 (br), 1024 (m), 1003 (m), 829 (w), 799 (w), 749 (w), 676 (w), 644 (w), 619 (w) cm^{-1}.

Scheme S1. Representation of the molecular structure of 2-chloro-4-(*N*,*N*-(2-pyridyl)amino)-6-(pentafluorophenoxy)-(1,3,5)triazine) (**L1**)

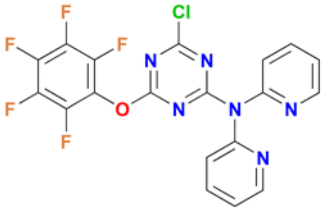

X-ray crystallography

Data for compound **1** were obtained at 100 and 200 K on the same crystal with a Bruker APEX II CCD diffractometer on the Advanced Light Source beamline 11.3.1 at Lawrence Berkeley National Laboratory, from a silicon 111 monochromator (λ = 0.7749 Å). Data reduction and absorption corrections were performed with SAINT and SADABS, respectively.[1] The molecular structure of **1** was solved and refined on F^2 using the SHELXTL suite.[2] Crystallographic and refinement parameters are summarized in Table S1. Selected bond distances and angles are given in Table S2. All details can be found in the supplementary crystallographic data for this paper in cif format with CCDC numbers 968835–968836. These data can be obtained free of charge from The Cambridge Crystallographic Data Centre via www.ccdc.cam.ac.uk/data_request/cif.

Differential Scanning Calorimetry (DSC)

DSC measurements were performed with a Q1000 calorimeter from TA Instruments equipped with the LNCS accessory. The temperature and enthalpy scales were calibrated with a standard sample of indium, using its melting transition (156.6 ºC, 3296 J mol^{-1}). The measurements were carried out using aluminium pans with a mechanical crimp, with an empty pan as reference. The zero-heat flow procedure described by TA Instruments was followed to derive heat capacities, using a synthetic sapphire as reference compound. An overall accuracy of ca. 0.2 K for the temperature and up to 5 to 10 % for the heat capacity was estimated over the whole temperature range, by comparison with the synthetic sapphire. A lattice heat capacity was estimated from data below and above the anomaly associated with the SCO process (dashed line in Figure S2). Excess enthalpy and entropy were derived by integration of the excess heat capacity with respect to *T* and Ln*T*, respectively.

Details of modelization of ΔC_p data with the so-called domain model.

The phenomenological domain model developed by Sorai[3-5] was applied here, as it is widely used to analyse the SCO behaviour in cases where calorimetric data are available. It is based on heterophase fluctuations and gives a measure of cooperativity through the number of like-spin molecules (or here the SCO centres) *n* per interacting domain, the larger the domain the more cooperative the transition. According to this model, the HS fractions can be written as:

$$\Delta C_p = \frac{n\left(\Delta_{SCO}H\right)^2}{RT^2} \frac{\exp\left[\frac{n\Delta_{SCO}H}{R}\left(\frac{1}{T}-\frac{1}{T_{SCO}}\right)\right]}{\left\{1+\exp\left[\frac{n\Delta_{SCO}H}{R}\left(\frac{1}{T}-\frac{1}{T_{SCO}}\right)\right]\right\}^2} \qquad \text{Eq. S1}$$

The experimental data were thus fitted to Eq. S1 using $\Delta_{SCO}H$ as derived from integration of ΔC_p vs. *T*, giving n = 14.2 and T_{SCO} = 129.9 K (full red line in Figure 2b). For n = 1 the model is equivalent to a pure solution behaviour (van't Hoff equation) with no cooperative effects.

Table S1. Crystallographic data for low-spin (LS) **1** and high-spin (HS) **1**.

Compound	LS **1**	HS **1**
Empirical formula	$C_{40}H_{16}Cl_2F_{10}FeN_{14}O_2S_2$, $2(CH_4O)$	$C_{40}H_{16}Cl_2F_{10}FeN_{14}O_2S_2$, $2(CH_4O)$
Formula weight	1169.62	1169.62
Crystal system	Triclinic	Triclinic
Crystal colour	purple	yellow
a (Å)	9.084(4)	9.173(2)
b (Å)	10.766(5)	11.167(3)
c (Å)	12.658(5)	12.759(3)
α (°)	96.115(6)	94.784(4)
β (°)	103.282(5)	105.483(3)
γ (°)	98.341(5)	100.902(3)
V (Å^3)	1179.4(9)	1224.4(5)
T (K)	100(2)	200(2)
Space group	*P*-1	*P*-1
Z	1	1
μ (mm^{-1})	0.781	0.752
Reflections collected	13506	13341
Unique reflections/R_{int}	5362/0.0438	4973/0.0361
R_1/wR_2/*S* (I/σ(I)>2)	0.0662/0.1700/1.042	0.0547/0.1519/1.039
R_1/wR_2/*S* (all data)	0.0866/0.1820/1.050	0.0741/0.1619/1.046
Residual ρ/e Å^{-3}	0.857 and –0.721	0.411 and –0.386
CCDC number	968835	968836

Table S2. Selected bond lengths (Å) and angles (°) for LS and HS **1**.[a]

LS **1**			
Bond lengths			
Fe1–N1	1.953(3)	Fe1–N2	2.005(3)
Fe1–N3	2.012(3)		
Angles			
N2–Fe1–N3	86.60(14)	N2–Fe1–N3a	93.40(14)
N1–Fe1–N1a	180.00		
HS **1**			
Bond lengths			
Fe1–N1	2.076(3)	Fe1–N2	2.221(3)
Fe1–N3	2.235(3)		
Angles			
N2–Fe1–N3	83.15(11)	N2–Fe1–N3a	96.85(11)
N1–Fe1–N1a	180.00		

[a] Symmetry operation: a = 1–x, 1–y, 1–z

Figure S1. Zoom of the χT vs. T data for **1** evidencing the presence of a 1 K hysteresis (that is reproducible). The measurements were performed at ca. 0.3 K/min.

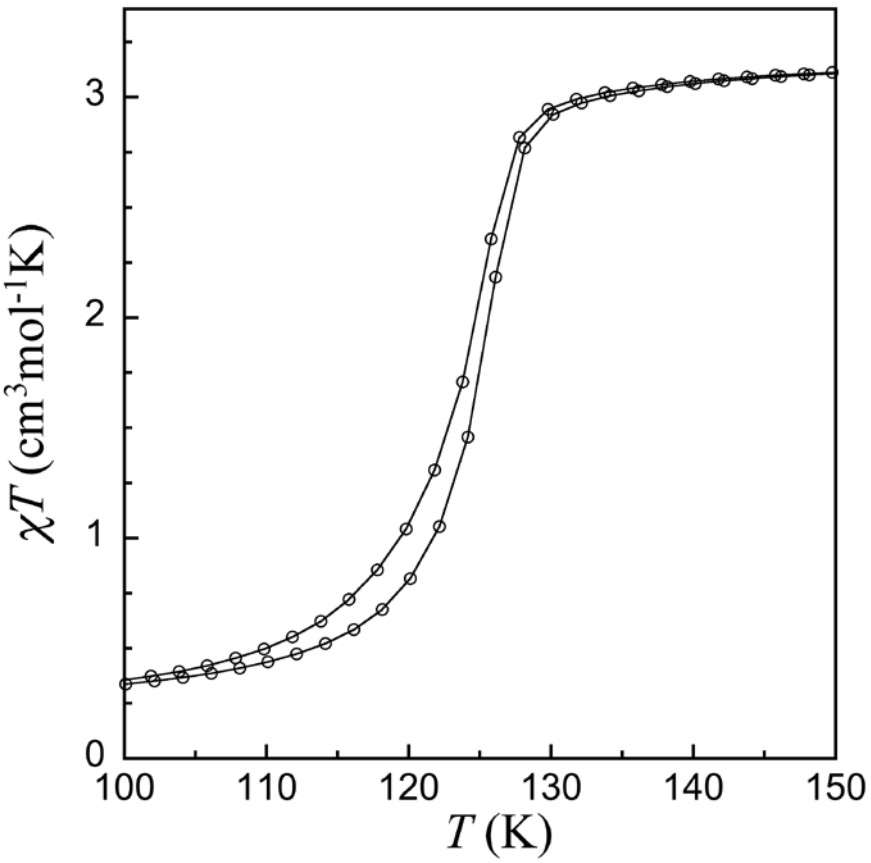

Figure S2. Molar heat capacities of **1** showing the sharp peak associated with the SCO. The dashed line is the estimated lattice component.

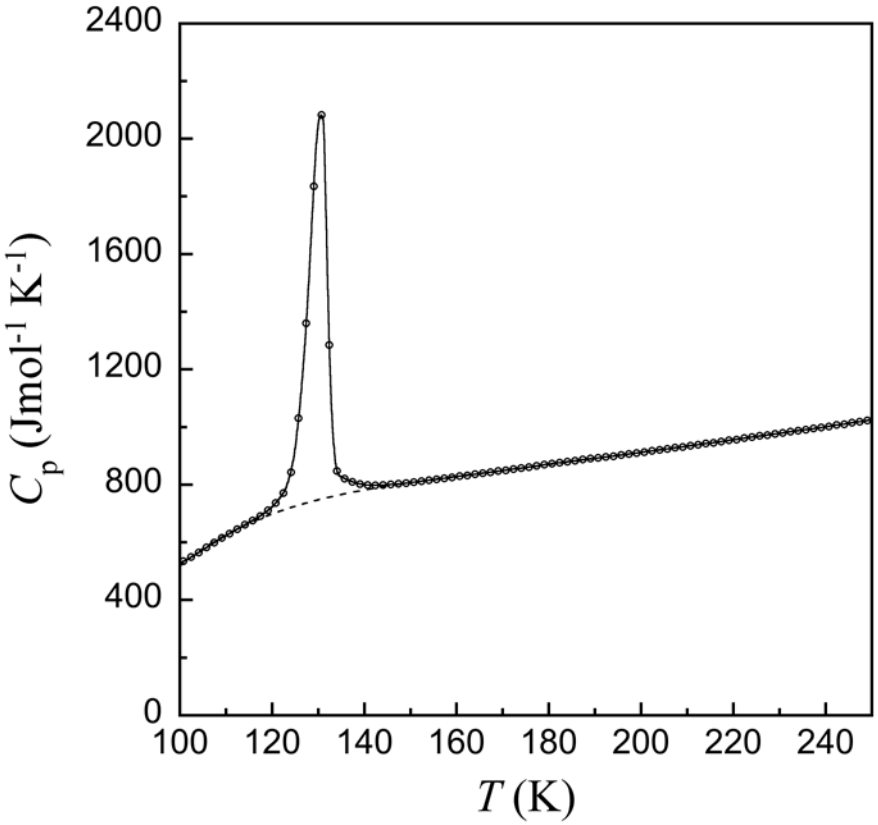

Figure S3. Excess enthalpy involved in the process of SCO in compound **1**, as derived from the integration of the ΔC_p data in the warming mode vs. *T*. The entropy in Figure 2b is obtained similarly by integration over Ln*T*.

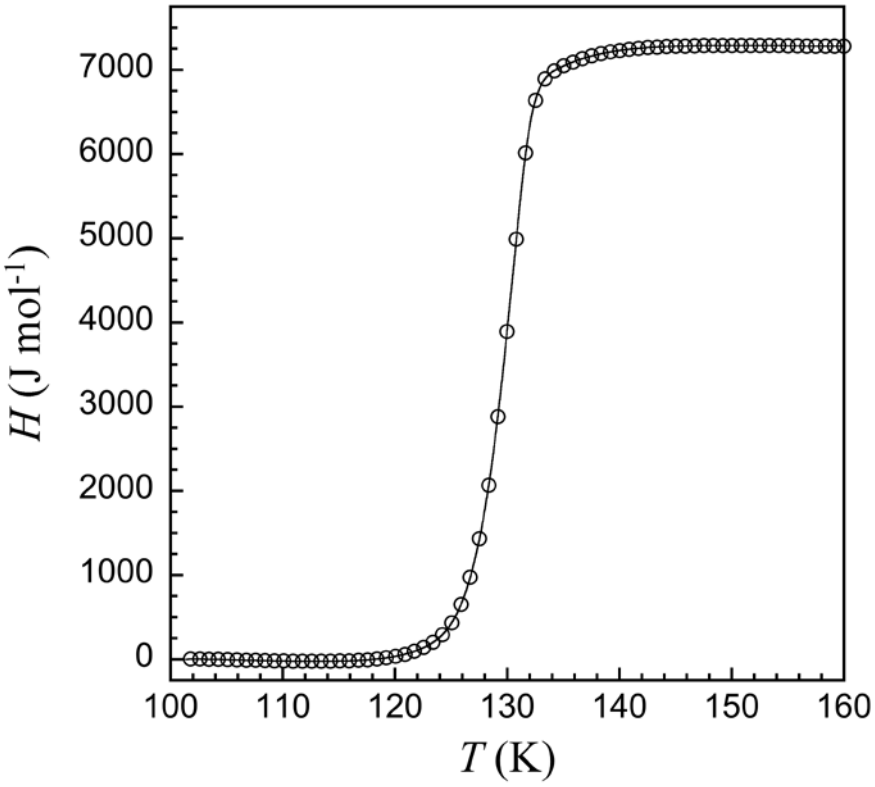

Table S3. Coordination parameters and supramolecular interactions for LS and HS **1**.

Compound	LS **1**	HS **1**
Coordination distortion parameters[6]		
ΣFe[a]	32	39
Φ[b]	42	64
π–π interactions[c]		
C18···F2j	3.076(6) Å	3.205(6) Å
S–π interactions (lone pair–π)[d]		
C16···S1h	3.382(5) Å	3.430(4) Å
C17···S1h	3.347(6) Å	3.393(5) Å
F2···S1h	3.269(4) Å	3.337(3) Å
O–π interactions (lone pair–π)[e]		
F5···O1n	2.922(4) Å	2.922(4) Å
C20···O1n	3.085(6) Å	3.166(5) Å
Halogen bonding[f]		
F3···Cl1k	2.969(4) Å	3.013(4) Å

[a] Σ = the sum of $|90 - \theta|$ for the 12 N–Fe–N angles in the octahedron. [b] Φ = the sum of $|60 - \theta|$ for the 24 N–Fe–N angles describing the trigonal twist angle. [c] see Figure S1. [d] see Figure S2. [e] see Figure S3. [f] see Figure S4. Symmetry operations: h = 1+x, y, 1+z; j = 2–x, 2–y, 2–z; k = 1+x, 1+y, z; n = 2–x, 1–y, 2–z.

Figure S4. Parallel-displaced π–π interactions between two neighbouring pentafluoro rings (F2···C18j = 3.076(6) Å for LS **1** and 3.205(6) Å for HS **1**) observed in the crystal packing of **1**. Symmetry operation: j = 2–x, 2–y, 2–z.

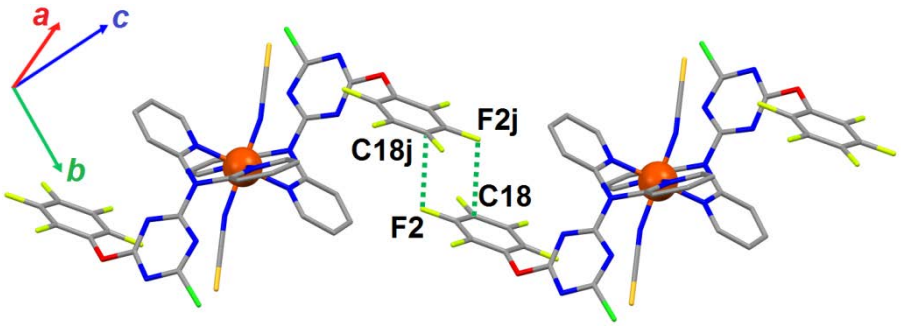

Figure S5. S–π interactions (lone pair–π) between a thiocyanate sulfur atom and one pentafluoro ring of an adjacent iron(II) complex (S1h···C16 = 3.382(5) Å, S1h···C17 = 3.347(6) Å and S1h···F2 = 3.269(4) Å for LS **1**) found in the crystal packing of **1**. Symmetry operation: h = 1+x, y, 1+z.

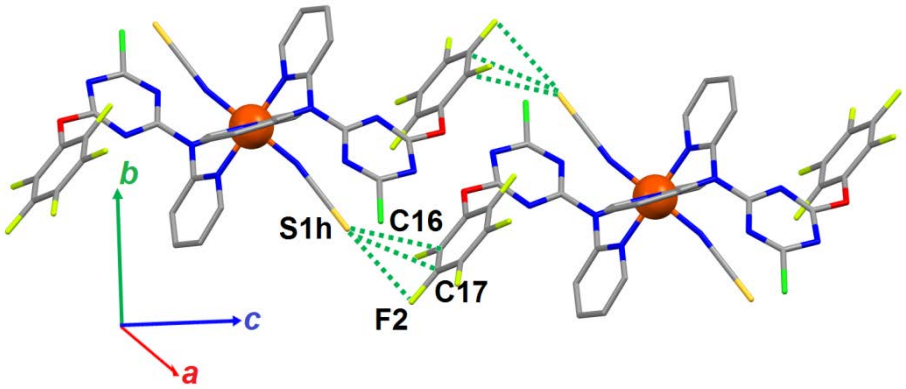

Figure S6. O–π interactions (lone pair–π) between two pentafluoro rings from two adjacent iron(II) complexes (O1n···F5 = 2.922(4) Å and O1n···C20 = 3.085(6) Å for LS **1**) observed in the solid-state structure of **1**. Symmetry operation: n = 2–x, 1–y, 2–z.

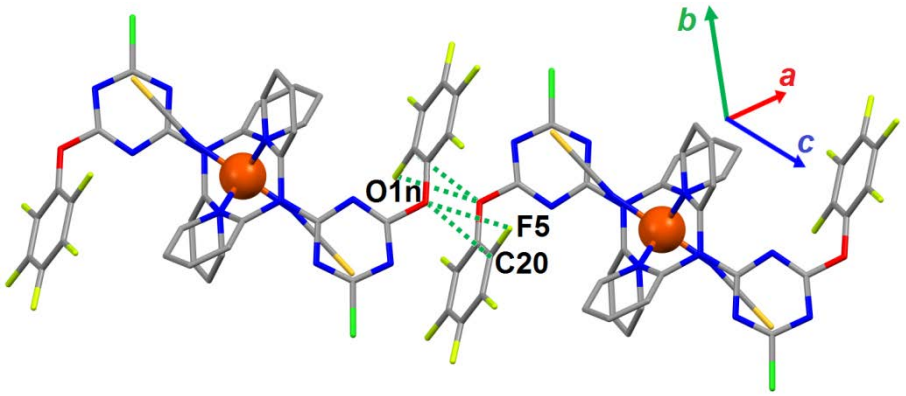

Figure S7. Halogen bonding between a fluorine atom of a pentafluoro ring and a chlorine atom from a neighbouring triazine moiety (F3···Cl1k = 2.969(4) Å for LS **1** and 3.013(4) Å for HS **1**). Symmetry operation: k = 1+x, 1+y, z.

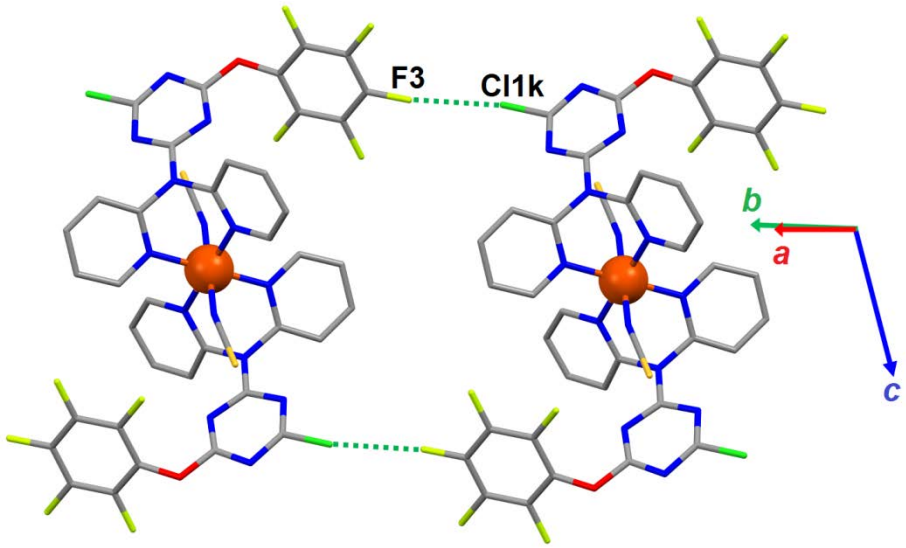

Figure S8. Crystal packing of **1** in the a) *bc* plane; b) *ac* plane and c) *ab* plane. The different Fe···Fe separation distances are given for LS **1**.

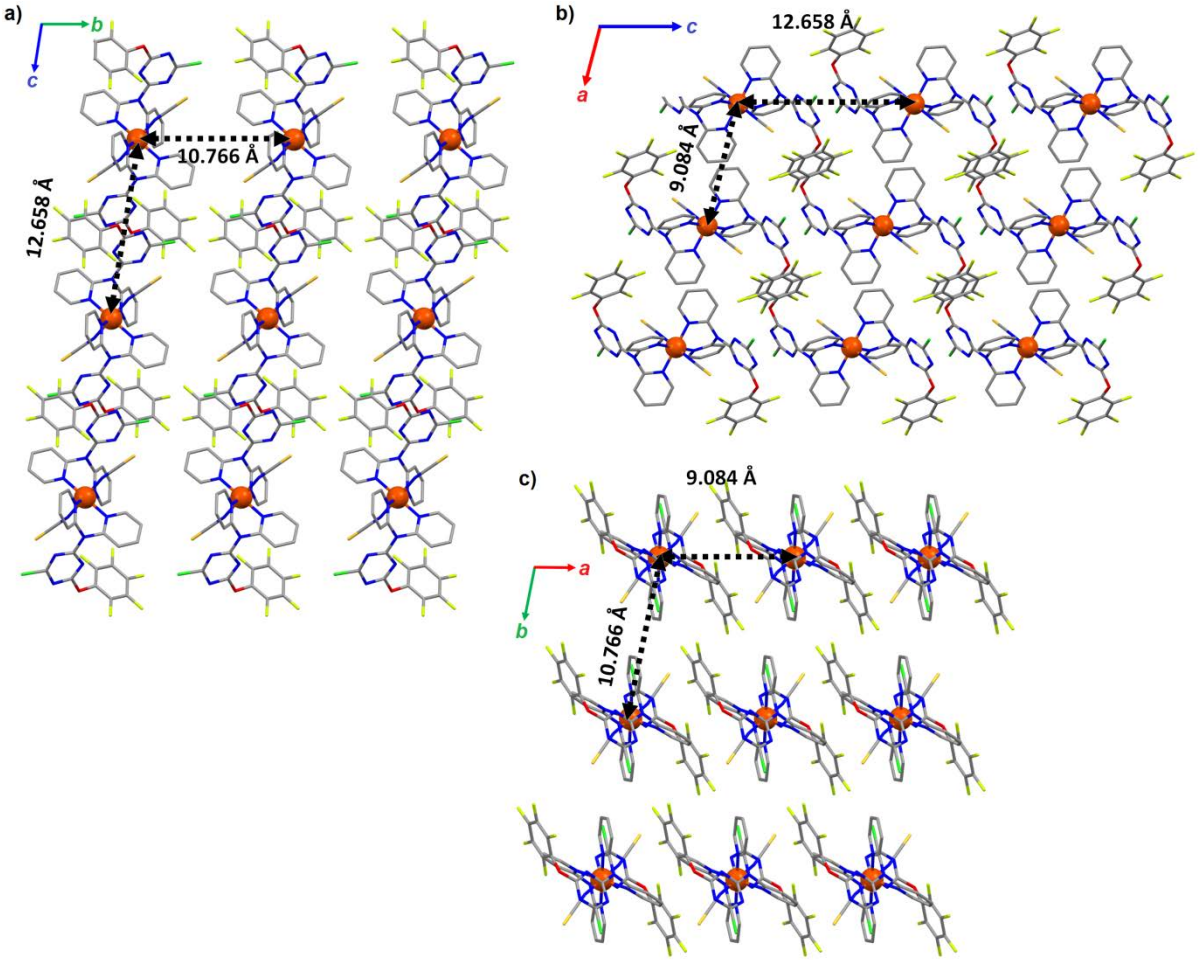

Table S4. Fe···Fe separation distances observed in the three different crystallographic axes of the solid state structure of **1**, and their variation upon LS ↔ HS transition.

Compound	Fe···Fe distances			Σ Fe···Fe distances
Direction	along *c*	along *b*	along *a*	
LS **1**	12.658 Å	10.766 Å	9.084 Å	32.508 Å
HS **1**	12.759 Å	11.167 Å	9.173 Å	33.099 Å
Variation	0.8 %	3.7%	1.0%	1.8%

Figure S9. a) Representation of the molecular structure of ligand 2-(*N*,*N*-bis(2-pyridyl)amino)-4,6-bis(pentafluorophenoxy)-(1,3,5)triazine (**L1**^{F}).[7] Crystal packing of *trans*-[Fe(**L1**^{F})$_2$(NCS)$_2$]·2CH$_3$CN (**2**)[7] in the b) *bc* plane; c) *ac* plane and d) *ab* plane. The different Fe···Fe separation distances are given for LS **2**.

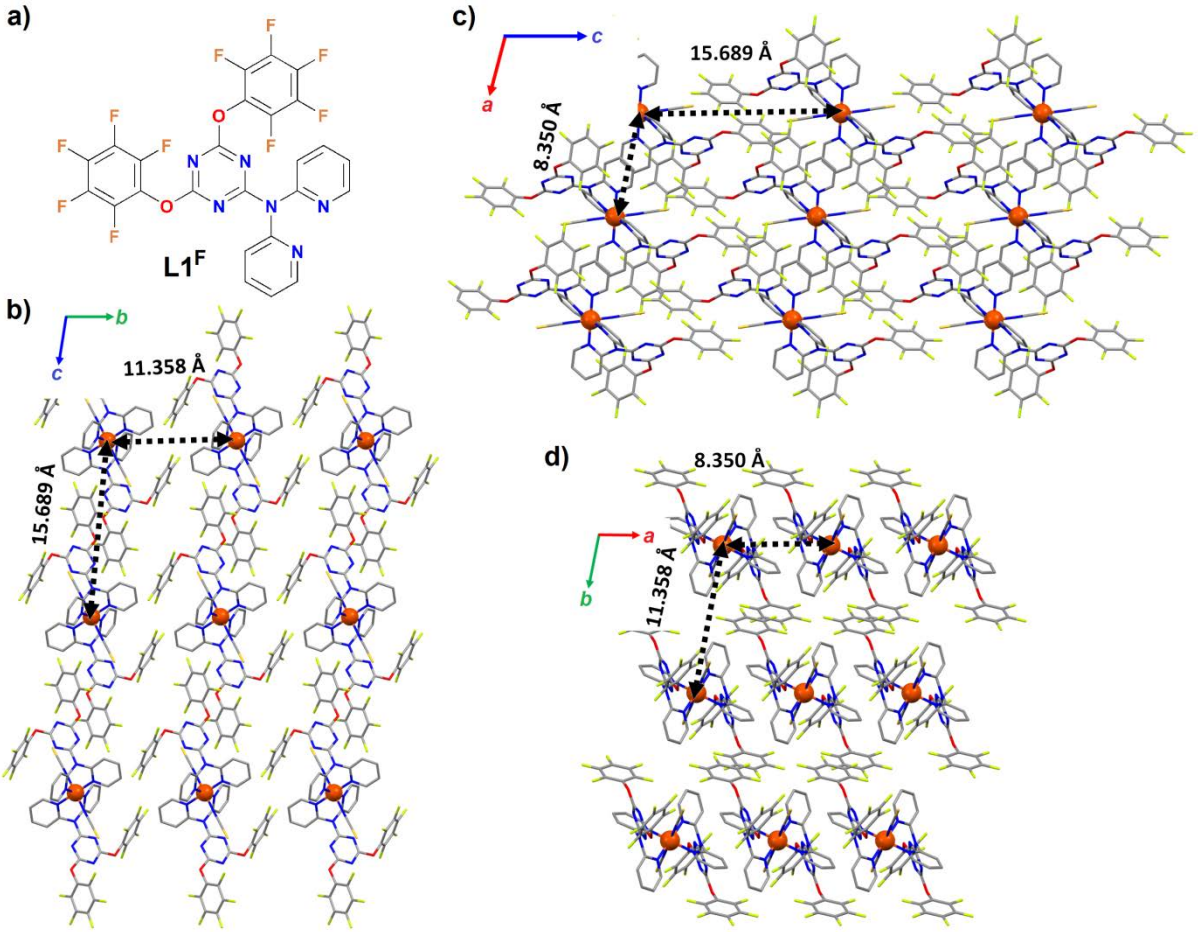

Table S5. Fe···Fe separation distances observed in the three different crystallographic axes of the solid state structure of **2**,[7] and their variation upon LS ↔ HS transition.

Compound	Fe···Fe distances			Σ Fe···Fe distances
Direction	along *c*	along *b*	along *a*	
LS **2**	15.689 Å	11.358 Å	8.350 Å	35.397
HS **2**	15.844 Å	11.494 Å	8.643 Å	35.981
Variation	1%	1.2%	3.5%	1.6%

References

1. *SAINT, SADABS and SHELXTL*, (2002) Bruker AXS, Inc., Madison, WI , USA.
2. G. M. Sheldrick, *Acta Crystallogr. Sect. A*, 2008, **64**, 112-122.
3. M. Sorai and S. Seki, *J. Phys. Chem. Solids*, 1974, **35**, 555-570.
4. M. Sorai, *Top. Curr. Chem.*, 2004, **235**, 153-170.
5. M. Sorai, M. Nakano and Y. Miyazaki, *Chem. Rev.*, 2006, **106**, 976-1031.
6. M. A. Halcrow, *Chem. Soc. Rev.*, 2011, **40**, 4119-4142.
7. N. Wannarit, O. Roubeau, S. Youngme, S. J. Teat and P. Gamez, *Dalton Trans.*, 2013, **42**, 7120-7130.